

An Undergraduate Course in Applied Magnetism

J. KENNETH WATSON, SENIOR MEMBER, IEEE

Abstract—This paper points out a need for better education in applied magnetism in order to serve a broad spectrum of electrical engineering interests. Described here is a proposed partial solution to this need, an undergraduate course that demonstrates the wide applicability of a few fundamental principles. Two introductory concepts of the course are the characterization of a magnetic device in units of volt-seconds versus current, and the definition of a piecewise linear magnetic model. These are illustrated by an example in the Appendix. The piecewise linear model provides a point of departure for the study of magnetic materials while also allowing some analytical relief to the empirical aspects of magnetism design.

INTRODUCTION

MAGNETICS applications thread through the practice of electrical engineering to a surprising extent, yet there exist few courses in the U.S. that deal in any comprehensive manner with the subject of applied magnetism [1]. Industrial groups have lamented the shortage of "magneticians" and have encouraged the introduction of more applied magnetism into our undergraduate curricula [2]. The Education Committee of the IEEE Magnetism Society has debated the question of whether to ask for a minimum competency for accreditation [3], but fell short of actually taking such a step. This paper is written as a suggested way [4] to bring this matter before a broader forum. I hope this article will convince some of the readers that both a need and an opportunity exist for the presentation of a course in applied magnetism in electrical engineering at the undergraduate level.

As examples of the ubiquity of magnetism, consider the following applications and note their diversity. Most computer memory of the nonvolatile type is magnetic, in the form of disks either rigid or floppy, tapes, or perhaps magnetic bubbles. Domain magnetism has emerged from laboratory obscurity to become an integrated circuit memory technology in which domains are moved, stretched, shrunk, or split with high reliability. Magnetic plated wire continues to be a viable random-access digital storage technology for harsh environments. Thin-film technology is being widely adapted to new applications, including magnetic heads for high-density data recording and reproduction. Switched mode dc to dc converters have revolutionized the design of dc power supplies by using efficient magnetic components, often in innovative configurations. Alternative energy sources offer new challenges for power process-

ing and magnetism. Sensitive magnetometers are used to chart geomagnetic and lunar fields, to search for mineral deposits, or to monitor the entrances into secure regions. Broad-band transformers and ferrite-loaded antennas have had an impact on the design of radio receivers. Rare-earth alloys and other new permanent magnet materials promise to open up new applications that require extremely high coercivity. Amorphous metallic alloys have now been added to the growing list of commercial magnetic materials that are available to design engineers. The list has previously included ferrites, pressed powder materials, permalloys, and silicon iron. Microwave magnetism provides such functions as tuneable resonance, variable delay, or directional coupling. In the category of systems to produce magnetic fields, there are increasingly varied applications that require high magnetic fields of specified gradient. Examples include enormous field strengths for materials research, configurations proposed for the magnetic confinement of plasmas for fusion energy, magnetic gradient separation processes for refining minerals or for separating solid wastes, and proposed tracks for high-speed ground transportation using magnetic levitation instead of wheels.

Even though the list above is by no means exhaustive, it is evident that modern applied magnetism possesses a breadth and scope that cuts across the entire discipline of electrical engineering. This very diversity has wrought an educational challenge: how to provide a magnetism background of sufficient breadth and depth to prepare electrical engineering students for work in the current technologies. At the University of Florida we have taken the position that modern applied magnetism is fundamental enough to electrical engineering to deserve its own course. A course of broad emphasis has been developed over the past decade or more at the University of Florida, was given at the California Institute of Technology in 1980-81, and is described in this paper. The next section briefly outlines the contents of the course; the final section of the paper comments on a magnetic model that has proved to be helpful in making the subject matter accessible. The use is demonstrated in the Appendix of two components of the model.

COURSE DESCRIPTION

The course has been developed at the senior/graduate level over a several year period as a four quarter-credit course, and presently is given as three semester credits. There is considerable emphasis on design-related homework assignments, with half the course grade earned in this

Manuscript received September 27, 1982; revised July 19, 1983. This work was supported by the National Science Foundation under Grant ECS-8111623.

The author is with the Department of Electrical Engineering, University of Florida, Gainesville, FL 32611.

manner. Course topics include the following items presented in roughly the order listed:

- MKS units and constitutive equations
- Magnetics design: a simple prototype
- Piecewise linear magnetic model
- Saturation: cause and effects
- Precession: a fundamental reversal process
- A lesson from core memory
- Transformers: transformation properties of dc to dc converter (Royer circuit)
- Design for H fields: current density considerations
- Permanent magnets: field modeling, static design with Ferromagnetism theory
- Magnetic anisotropy: effect on B - H curve
- Inductance applications
- Switched-mode regulated power supply (Buck converter)
- Core losses, eddy currents
- Core reversal by domain wall motion
- Transformers: leakage inductance of, broad-band, ferro-resonant
- Tape recording and reproduction
- Exchange energy and domain wall thickness
- Permalloy thin films
- Bubble memory: introduction to

Since the course assumes no prior exposure to the physics of magnetic materials, basic principles of that subject are developed in an orderly manner throughout the term. It has proved to be a successful strategy to introduce a magnetic material concept and then to follow with an application that depends critically on that concept. For instance, the third item of the above list is a piecewise linear magnetic model. One component of the suggested model is saturation, which is interpreted at the atomic level, and the effects of which subsequently are identified in the core memory and then in the design of a dc to dc converter. Thus, the same magnetic phenomenon may link five or six nearby topics of the list above. Repetition of the same strategy for different phenomena gradually builds up the needed background of the physics of magnetic materials. In fact, a predominant principle of the course is to treat magnetic properties in a direct context of their applications [5]. For students who are interested in further study, excellent treatments of magnetic materials are available from the perspective of the metallurgist [6] or of the physicist [7]. Advanced books in various specialties are also available [9]–[15].

A PERSPECTIVE FOR MAGNETIC DESIGN

A prototype design process for core devices has been described [8] as involving four classes of decisions: choices of magnetic material, core geometry, turns of wire, and packaging which is not treated in the course. Material selection could involve specifying magnetic material parameters, or alternatively as choosing a magnetization curve of B versus H . Specification of core geometry carries the implication that the point variable of induction B will be integrated over the core cross section to yield magnetic flux ϕ , and that

field strength H will be integrated around the flux path of the core to yield magnetic potential F . In the simplest case of a toroidal core with no airgap, a graph of B versus H may be translated into a similar graph of $\phi = \overline{B}S$ versus $F = \overline{H}l$, simply by redefining the vertical and horizontal axes. The underbar denotes average value, S is core area, and l is mean path length. Choosing the number of turns n for the device may be interpreted similarly as multiplying $n\phi = \Lambda$ and dividing $F/n = i$ to yield a graph of the electrical characteristics, volt-seconds versus current, assuming MKS units are used. A slope on the latter characteristic has dimensions of inductance in henrys. The central concept is that core dimensions and turns serve to translate magnetic material properties into electrical properties as indicated by the above application of Faraday's and Ampere's laws, respectively.

The representation of a magnetic device by a graph of volt-seconds versus amperes communicates an insight to many students that most of them have previously lacked. It illustrates a very fundamental concept that helps open up magnetics design to those who are aware of it. The extension of this principle to include more complicated core geometries is easily shown later in the course. An example is given in the Appendix of this paper.

MAGNETIC MODELING

The modeling of magnetic materials and devices may play a vital role in a course that emphasizes electrical design. It is often true that design involves a synthesis that may include many areas such as mathematical analysis, device functional requirement, packaging, and costs. The characterization of magnetic materials may be only one of several design considerations in such an environment, so that even a crude characterization may provide a very helpful tool for design.

However, the characterization of magnetic materials has been largely empirical, usually based on experimental data supplied in the catalogs of core manufacturers, and often in the form of graphs of B versus H . Although each separate axis B or H may be translated into Λ or I by well-defined design procedures as pointed out in a paragraph above, the constitutive relation *between* the two axes B and H remains empirical. The empirical constraints to magnetic design may be relieved in many cases by the use of a modeling methodology.

A piecewise linear magnetic model for $B(H)$ is used in the course as a main vehicle for design and for beginning the study of magnetic materials [5]. By defining the constitutive relation between B and H , an analytical emphasis emerges that lends itself in many cases to the clear definition of design criteria and fundamental limitations. Most of the empirical aspects of magnetic design may be postponed or may be interpreted as departures from the simplest models. The model consists of four components: saturation, static coercivity, permeability, and dynamic increase in coercivity, each of which may be represented ideally by straight line segments as in Fig. 1. For sufficiently large H and with the assumption that $|B|$ is less than its saturation value, the four components may be merged into a single equation.

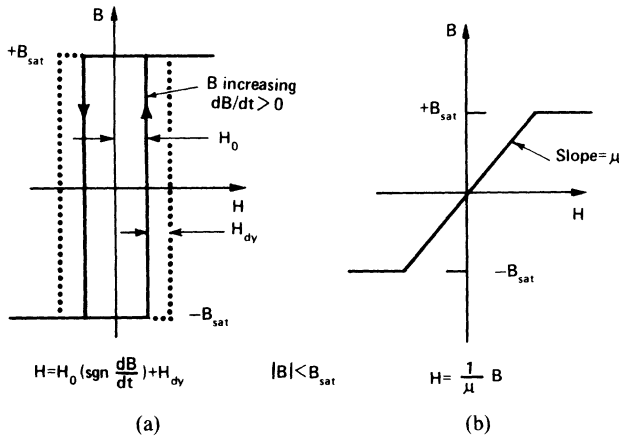


Fig. 1. Four components of piecewise linear model for magnetic materials: saturation flux density B_{sat} ; static width H_0 ; slope μ ; dynamic width H_{dy} . (a) Ideal square-loop core. (b) Ideal linear core.

$$H = H_0 \left(\text{sgn} \frac{dB}{dt} \right) + \frac{1}{\mu} B + g_e \frac{dB}{dt} \quad |B| < B_{sat} \quad (1)$$

In (1), H_0 is defined as static coercivity, $\text{sgn } dB/dt$ is either ± 1 as B increases or decreases with time, μ is an ideal permeability or slope parameter, and $g_e dB/dt$ is an approximation to the well-known phenomenon that hysteresis loops may be wider when measured at higher frequency. The essential features of a great many magnetic materials may be represented by values for the material constants B_{sat} , H_0 , μ , and g_e . In fact, the value of B_{sat} depends on the material composition, whereas H_0 , μ , and g_e may depend also on the material processing and geometry. Evidently g_e also varies to some extent with the magnetic reversal process that may be excited by the type of applied signal. In summary, (1) has the merit of giving an overall perspective of the relative effects of material parameters each of which may be explored in more detail, and has the additional merit of providing a reasonable model for certain materials.

An earlier paragraph has described a design procedure for translating magnetic quantities into electrical. A similar procedure can be done on (1) to convert the equation in H to the following equation in current:

$$I = I_0 (\text{sgn } v) + \frac{1}{L} \int v dt + G_e v \quad |\phi| < \phi_{sat} \quad (2)$$

which can be interpreted electrically as in Fig. 2. Fig. 2 is similar to the "equivalent circuits" that have been used for at least 40 years [16] to represent magnetic core responses, obtained by intuitive and empirical methods. The present model differs in its analytical derivation, by its generalization to square-loop cores and by including a provision for core saturation. It is interesting to note that the foregoing core model when extended to more complicated core geometries—to include an airgap in the flux path, conditions of current density, and leakage inductances—has been found adequate [5] to describe the essential features of a great variety of magnetic circuits including their design considerations.

Although there is no space here to describe them in detail, the course also includes other analogs to illustrate the

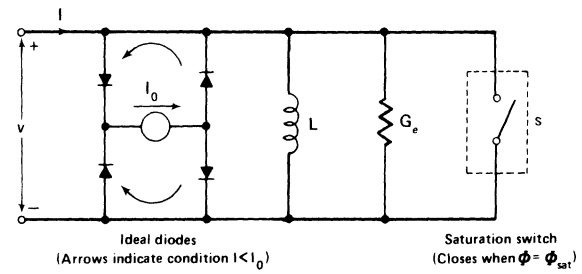


Fig. 2. Electrical version of piecewise linear model of the core of a magnetic device.

essential features of other magnetic phenomena. These include the orientation polarization of the dipole moment of certain dielectrics as analogous to magnetization processes; a spinning top in a gravitational field to explain the precessional motion of electron spins in an H -field; use of positive feedback to explain the concept of ferromagnetic interaction; and the use of negative feedback to analyze demagnetizing effects.

CONCLUDING COMMENTS

This paper has argued first of all that applied magnetism includes a comprehensive array of subjects to which electrical engineers need access. Underlying this diverse collection of topics is a set of common fundamental principles that can be exposed in an undergraduate course. Such a broadly based course exists at the University of Florida (EEL 4479, Applications of Magnetism) developed over the past decade or more, and was given at the California Institute of Technology in 1980–81 as EE 127.

The course brings together excerpts from circuits, electromagnetic field theory, and physics of materials in the context of practical design examples. A major pedagogical device of the course is a piecewise linear magnetic model which partially relieves the empirical constraints of this subject. Additional models and analogs are used to illustrate various magnetic phenomena. The author will be pleased to correspond with colleagues who are interested in magnetism education.

APPENDIX

This Appendix, written in response to a reviewer's suggestion, demonstrates the use of piecewise linear magnetic modeling in the analysis of a simple circuit.

Current and voltage waveforms are given for a series resistor-inductor circuit driven by a sinusoidal voltage, in which the inductor is driven into saturation. Both calculated and measured waveforms are given and may be compared to one another in order to demonstrate the methodologies and their limitations.

The calculations assume a piecewise linear model for the inductor, shown in Fig. 3. In the physical circuit, Fig. 4, an airgapped pot core is used to achieve inductor linearity below saturation. A differential measurement technique is used to subtract away the resistive component of the inductor voltage to facilitate comparison to calculations. Calculations and measurements were made at 60 Hz using parameter values given in Figs. 3 and 4 and in Table I.

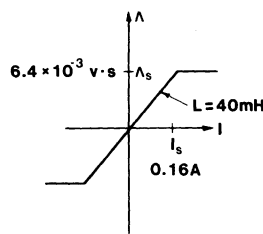


Fig. 3. Magnetization curve of ideal inductor.

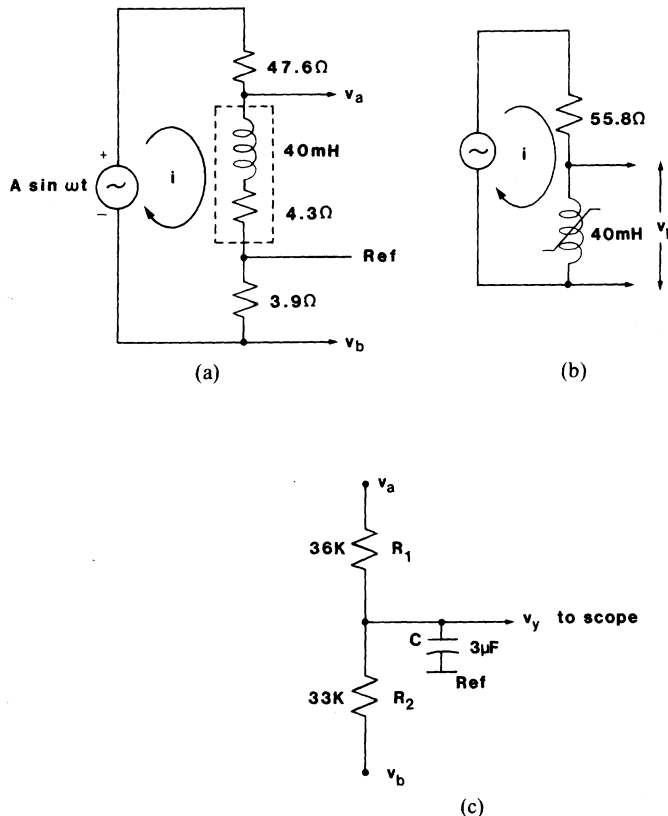


Fig. 4. (a) Physical circuit used for measurement. (b) Simplified circuit used for calculation. (c) Integration circuit added for measuring magnetization curve.

TABLE I

$I_1 = 0.367 \text{ A}$	$L = 40 \text{ mH}$
$I_2 \angle \theta_1 = 0.363 \text{ A} \angle 0.264 \text{ rad}$	$R = 55.8 \Omega$
$I_s = 0.16 \text{ A}$	$A = 21 \text{ V}$
$\lambda_s = 6.4 \times 10^{-3} \text{ V}\cdot\text{s}$	$f = 60 \text{ Hz}$
	$\sin \theta_2 = I_s/I_2$

CALCULATION OF CURRENT WAVEFORM

Since the inductor is isolated from the voltage source by a resistance, Fig. 4, the solution for the circuit is nontrivial because we do not know whether or not the inductor is saturated. The first task is to make that determination in order to know what inductor model to use.

From Fig. 2 of the main paper, we choose L in parallel with the saturation switch as our working model. If the

switch were always closed, the current would be in phase with the applied voltage $A \sin \omega t$, as

$$i_1(t) = I_1 \sin \omega t \quad (\text{A-1})$$

where $I_1 = A/R$. If the switch were always open, the current would lag the input voltage by phase angle $\theta_1 = \tan^{-1} \omega L/R$, as

$$i_2(t) = I_2 \sin(\omega t - \theta_1) \quad (\text{A-2})$$

where $I_2 = A/|Z|$ and $Z = R + j\omega L$. Both currents i_1 and i_2 are plotted in Fig. 5 with dotted lines. Now if peak amplitude I_2 exceeds the saturation value I_s defined in Fig. 3, which it does in this example, we may conclude that the inductor will be driven to saturation during each half cycle. Under such conditions the current waveform solution consists of selected segments of the limiting waveforms $i_1(t)$ and $i_2(t)$ plus additional segments that represent transitions between i_1 and i_2 . Referring to the upper part of Fig. 5, let us assume that at time t_1 the inductor current is crossing zero on the i_2 waveform. Subsequently, at time t_2 current i_2 reaches the value I_s at which the saturation switch closes at the phase angle $\theta_2 = \sin^{-1} I_s/I_2$. Hence, at t_2 the current suddenly jumps from the i_2 waveform to the i_1 waveform. The inductor remains saturated as long as the current exceeds I_s , i.e., from t_2 to t_3 in Fig. 5. At $t = t_3$, current i_1 has decreased to I_s , which implies that the saturation switch is to open. For $t \geq t_3$, the current is

$$i(t) = I_x e^{-(t-t_3)/\tau} + I_2 \sin(\omega t - \theta_1) \quad (\text{A-3})$$

which may be solved at $t = t_3$ to find

$$I_x = I_1 \sin \omega t_3 - I_2 \sin(\omega t_3 - \theta_1) \quad (\text{A-4})$$

which is a negative value since $I_1 \sin \omega t_3 = I_s$. In (A-3) time constant $\tau = L/R$; the decaying transient format of the first term is required by the boundary condition of current continuity at $t = t_3$ where the inductor comes out of saturation. At that corresponding time in other half cycles, that is, for $t = (t_3 \pm n\pi/\omega)$ where n is an integer, there must be an adjustment of the reference time of the transient term.

CALCULATION OF VOLTAGE WAVEFORM

Referring again to the upper part of Fig. 5, consider now the waveform of $\Lambda(t)$ which is coincident with the current waveform when $|i| < I_s$. The coincidence is permissible since i and Λ are linearly related according to Fig. 3. However, for current greater than I_s , the flux linkage remains constant at λ_s as shown by the horizontal dashed line from t_2 to t_3 in Fig. 5. The constant flux, which has zero time derivative and hence must yield zero induced voltage according to Faraday's law, is the physical process that is summarized as a "closed saturation switch."

It is useful to recognize that the induced voltage is given by the time derivative of the flux linkage

$$v = \frac{d\Lambda}{dt} \quad (\text{A-5})$$

where for an ideal linear inductor the flux linkage may be defined as

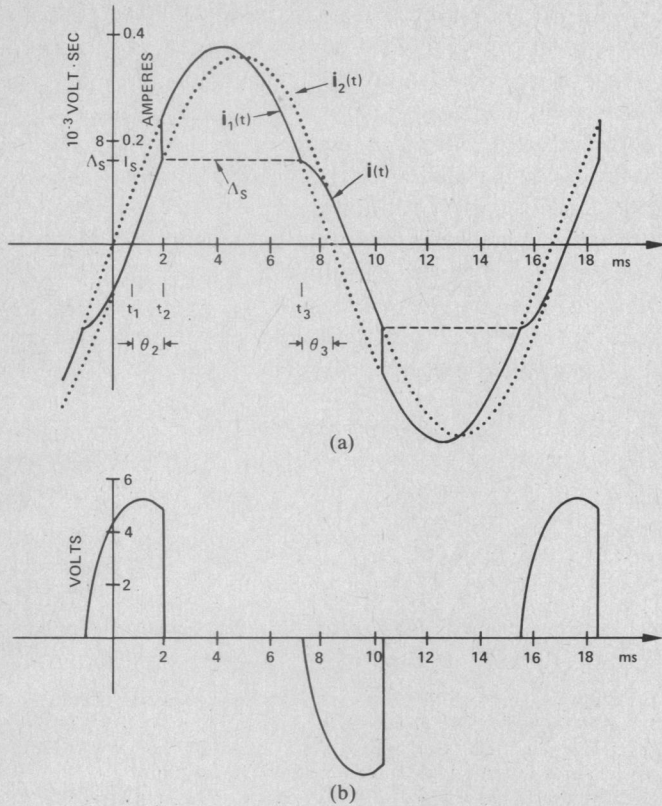


Fig. 5. (a) Current and flux-linkage waveforms. (b) Voltage waveform, calculated for circuit of Fig. 4. The current waveform is a composite of sinusoids $i_1(t)$ and $i_2(t)$ plus transitions between the two. See text for details.

$$\Lambda = n \Phi = n B S_c = L i. \quad (\text{A-6})$$

The application of Faraday's law in the form of (A-5) may avoid some possible confusion when analyzing a circuit in which both L and i are time varying. According to the model, the induced voltage is zero for the time period $t_2 < t < t_3$, but for $t \geq t_3$ the voltage may be found from the derivative of (A-3) as

$$v(t) = -I_x R e^{-(t-t_3)/\tau} + \omega L I_2 \cos(\omega t - \theta_1). \quad (\text{A-7})$$

It can be shown that the integral of (A-7) is

$$\int_{t_3}^{t_2+\pi/\omega} v(t) dt = -2 L I_s \text{ V} \cdot \text{s} \quad (\text{A-8})$$

as expected from Fig. 3, indicating that the area under one voltage pulse may drive the core from one polarity of saturation to the other.

The circuit parameters used in the calculations are summarized in Table I.

MEASURED WAVEFORMS

Fig. 6 shows the experimental waveforms of current and of induced voltage which may be compared to the calculated waveforms of Fig. 5. The value of saturation current was judged to be about 0.16 A from the current waveform, and that value was used in the calculations. The similarities are notable for the general waveform features and for the

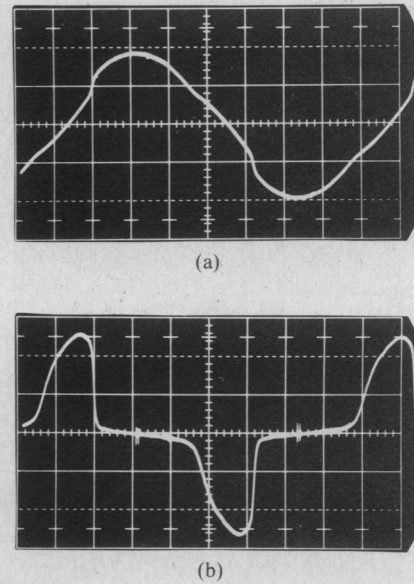


Fig. 6. (a) Current and (b) voltage waveforms measured for circuit of Fig. 4. The current scale is 0.2 A/div and the voltage scale is 2 V/div. Both time scales are 2 ms/div and are in phase.

respective amplitudes. The evident discrepancies are the slower transitions of the measured quantities and also the nonzero slope between the voltage pulses. Both features may be attributed to a finite saturation inductance of the core, judged from Fig. 6 to be about 4 mH.

In Fig. 6(b), the area under one voltage pulse is about 3 squares, at $4 \times 10^{-3} \text{ V} \cdot \text{s}$ per square which is the right order. The voltage waveform was found by subtracting the resistance portion from the total coil voltage; i.e., the scope display is explained in Fig. 4 as

$$v = v_a + k v_b \quad (\text{A-9})$$

where k is the variable gain of the second channel when the scope is used as a summing amplifier.

MEASURED MAGNETIZATION CURVE

Magnetization curves of flux-linkage versus current have been obtained experimentally for the inductor, Fig. 7. Approximate values of current and flux linkage at the onset of core saturation were found to be 0.16 A and $6.4 \times 10^{-3} \text{ V} \cdot \text{s}$, respectively, corresponding to $L = 40 \text{ mH}$. The transition from linearity to saturation may be noted to be somewhat rounded, and some hysteresis is observed for the case of a large drive signal. Interestingly, the hysteresis effect appears as a vertical separation of about $9 \times 10^{-4} \text{ V} \cdot \text{s}$, an amount that varies with excess drive.

The scope display of the integral of inductor voltage was obtained using a passive RC integrator with an auxiliary resistance network to cancel the resistive component of the voltage drop of the inductor winding; see Fig. 4(c). It may be easily shown that

$$\int v_L dt = R_l C v_y \quad (\text{A-10})$$

so that in Fig. 7 the vertical scale factor of $4.3 \times 10^{-3} \text{ V} \cdot \text{s}/$

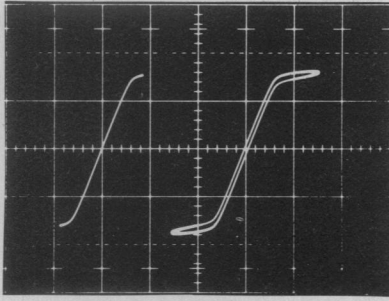


Fig. 7. Magnetization curves measured for two levels of current drive. The vertical scale is $4.3 \times 10^{-3} \text{ V} \cdot \text{s/div}$ and the horizontal scale is $2/7 \text{ A/div}$.

div equals $36\text{K} \times 3 \mu\text{F} \times$ the scope sensitivity of 40 mV/div . Equation (A-10) is valid only in the frequency range such that $\omega R'C \gg 1$ where $R' = R_1 R_2 / (R_1 + R_2)$. Aside from the integrator, the circuit and signal source were the same as used for waveform observations; the signal source was an isolation transformer supplied by a variable autotransformer connected to line voltage.

INDUCTOR CONSIDERATIONS

The inductor was realized using a ferrite pot core (Ferroxcube 2213, 3B7 material) with an airgap. One half of the pot core was commercially gapped (PA 250), but the other half was ungapped (PL00) in order to increase the permeance from 250 nH/t^2 . This particular combination was just a matter of expediency in using cores that were at hand. Higher permeance than 250 was thought to be needed in order that the current density would not be excessive when driving the core to saturation. Yet on the other hand, the permeance needed to be dominated by an airgap in order that the inductor would be linear. At 40 mH inductance for 295 turns the permeance is 460 nH/t^2 ; at the saturation current of 0.16 A in AWG #30 wire the current density is about 300 A/cm^2 . The temperature rise was not excessive even during waveform observations when the peak current was nearly 0.4 A . In retrospect I might have used a smaller value of R to increase the θ_1 phase shift.

The saturation flux linkage of $6.4 \times 10^{-3} \text{ V} \cdot \text{s}$ in Fig. 3 may be confirmed roughly as $\Lambda_s = n B_s S_c = 295 \times 0.42 \times 0.51 \times 10^{-4} = 6.3 \times 10^{-3}$ using 0.42 T as the approximate saturation induction and using the nominal cross section $S_c = 0.51 \text{ cm}^2$ of the center post of the pot core. Assuming the permeance of the core is dominated by an airgap of the same area as the center post yields $l_g = 139 \mu\text{m}$ as the estimated gap length. This now permits the current at saturation to be estimated, using

$$I_s = \frac{B_s l_g}{\mu_o n} \quad (\text{A-11})$$

The result, $I_s = 0.16 \text{ A}$, confirms the measured value estimated from the current waveform, Fig. 6, and from the magnetization curve, Fig. 7.

CONCLUSION

This Appendix has demonstrated the use of piecewise linear magnetic modeling to calculate current and voltage

waveforms. The waveforms are for a simple series resistance and saturating inductance circuit driven by a sinusoidal voltage source. The solution to this problem is believed to be a new result, and corrects an error on p. 59 of [5].

An inductor has been designed to approximate the piecework linear model for this problem, which was originally conceived as a fictitious example. Current and voltage waveforms have been measured experimentally and have been compared to the calculations for the same circuit, showing both qualitative and quantitative similarities. The agreement is judged to be satisfactory since no special care was taken to use precision components.

ACKNOWLEDGMENT

Several helpful conversations with J. R. O'Malley are gratefully acknowledged. The author also thanks C. Strukely for help with measurements.

REFERENCES

- [1] L. A. Finzi and F. J. Friedlaender, "Magnetics in the undergraduate electrical engineering curriculum," *Proc. IEEE*, vol. 59, pp. 996-998, June 1971.
- [2] S. Zwass, Los Angeles Chapter, IEEE Magnetics Society, letter, Nov. 3, 1981.
- [3] IEEE Mag. Soc. Meet. MMM Conf., Atlanta, GA, Nov. 11, 1981.
- [4] E. Della Torre, private communication, Dec. 1981.
- [5] J. K. Watson, *Applications of Magnetism*. New York: Wiley, 1980.
- [6] B. D. Cullity, *Introduction to Magnetic Materials*. Reading, MA: Addison-Wesley, 1972.
- [7] S. Chikazumi, *Physics of Magnetism*. New York: Wiley, 1964.
- [8] J. K. Watson, "Design with magnetic materials," in *Encyclopedia of Materials Science and Engineering*, M. B. Beuer, Ed. Elmsford, N.Y.: Pergamon, to be published.
- [9] R. Lee, *Electronic Transformers and Circuits*, 2nd ed. New York: Wiley, 1955.
- [10] C.W.T. McLyman, *Transformer and Inductor Design Handbook*. New York: Marcel Dekker, 1978.
- [11] R. J. Parker and R. J. Studders, *Permanent Magnets and Their Application*. New York: Wiley, 1962.
- [12] H. F. Storm, *Magnetic Amplifiers*. New York: Wiley, 1955.
- [13] M. Prutton, *Thin Ferromagnetic Films*. London: Butterworths, 1964.
- [14] C. D. Mee, *The Physics of Magnetic Recording*. Amsterdam: North Holland, 1964.
- [15] A. H. Eschenfelder, *Magnetic Bubble Technology*. Berlin: Springer-Verlag, 1980.
- [16] M.I.T. Staff, *Magnetic Circuits and Transformers*. New York: M.I.T. Press and Wiley, 1943.



J. Kenneth Watson (S'53-M'55-SM'61) was born in Ada, OK, on September 23, 1929. He received the B.S.E.E. degree from the University of Oklahoma, Norman, in 1951, the S.M. degree from the Massachusetts Institute of Technology, Cambridge, in 1955, and the Ph.D. from Rice University, Houston, TX in 1966.

He has been on the faculty of University of Florida since 1966 where he is currently Professor of Electrical Engineering. His prior experience includes five years in industry followed by eight years of digital computer engineering at the University of Oklahoma and at Rice University. He has taken sabbatical leaves at the Navy's White Oak Laboratory, MD, in 1972-1973 where he worked on the cross-tie memory, and at the California Institute of Technology, Pasadena, in 1980-1981 where he worked in power electronics. He is presently interested in various aspects of applied magnetism, both research and teaching.